SUPERMASSIVE BLACK HOLES IN THE UNIVERSE

ANDREAS BRUNTHALER AND HEINO FALCKE
Max-Planck-Institut für Radioastronomie
Auf dem Hügel 69, 53121 Bonn, Germany

Abstract. In these lecture notes we will give a very basic introduction to supermassive black holes. We derive the basic luminosity expected for accretion and introduce the Eddington limit. Kinematical evidence for black holes in the centers of galaxies from optical and radio spectroscopy is discussed as well as the link between black holes and host galaxy properties. Finally we consider the evidence for the black hole in the Galactic Center.

1. Introduction

In the early sixties, a number of strong radio sources were detected that were associated with optical point sources. Although they appear stellar on photographic plates, they had very strange optical emission lines which were different from anything seen before in stars. Schmidt (1963) realized for one of this "quasi stellar radio sources" (quasars), 3C 273, that the emission lines can be explained with hydrogen emission at a redshift of $z = 0.158$.

This unusual high redshift lead to another problem. The optical brightness of $m_B = 13.1$ corresponds to a luminosity of $L = 2 \times 10^{46}$ erg s^{-1} or 0.5×10^{13} L$_\odot$. Since the sources show variability on timescales of less than a year, the size of the emitting region is restricted to be smaller than one light year. Although confined into a 10^{-12}th fraction of the volume of a galaxy, the luminosities of these quasars exceed the luminosity of an entire galaxy. The most efficient way to release energy is accretion in a deep, relativistic gravitational potential. Only supermassive black holes have survived today as major paradigm to explain the huge energy output of the central engine of active galactic nuclei.

The next chapter will give a very basic introduction into the accretion of black holes. In chapter 3 we will review some evidence for supermassive black holes in external galaxies, while chapter 4 will focus on the black hole in our Galactic Center.

2. Black Holes – Basic Principles

A key feature of general relativity is that the presence of mass distorts space-time. In a black hole the space-time is curved to such an extend that light can no longer escape. The characteristic size of a black hole is given by its Schwarzschild radius. This radius is in classical terms the radius at which the escape velocity is equal to the speed of light:

$$v_{esc} = \sqrt{\frac{2GM}{R}} = c \;\Rightarrow\; R_S = \frac{2GM_{BH}}{c^2} = 3\ \mathrm{km} \times \frac{M_{BH}}{\mathrm{M}_\odot}. \tag{1}$$

Any material or radiation that falls into this event horizon is trapped forever in the black hole.

2.1. ACCRETION

The strong gravity field of the black hole will attract gas clouds in the central region of its host galaxy. This gas clouds will collide with each other in the vicinity of the black hole and transform kinetic energy into frictional heating. Usually the gas clouds will have a certain amount of angular momentum which has to be conserved. This will lead to the formation of an accretion disk. The particles in the disk will continue to interact with each other and heat the disk even more. In this process the particles will lose kinetic energy and move inwards while angular momentum is transported outwards, until the gas finally reaches the last stable orbit and falls into the black hole. The heated accretion disk will radiate predominantly in the optical and UV and produce the enormous luminosities observed in quasars.

The energy output is related to the rate of accreted material. A particle with mass m which falls in a gravitational potential of a central mass M from an infinite distance to a distance R from the black hole gains the energy:

$$U = \frac{GMm}{R}. \tag{2}$$

In the case of a black hole, the accreted material can only radiate until it reaches the event horizon R_S. If the energy is converted with an efficiency of η into radiation, the luminosity depends on the accretion rate $\dot{m}$ as:

$$L = \eta \dot{U} = \eta \frac{GM_{BH}}{R_S}\frac{dm}{dt} = \eta \frac{1}{2}\dot{m}c^2 \tag{3}$$

or

$$L = 10^{46}\frac{\mathrm{erg}}{\mathrm{s}}\left(\frac{\eta}{0.1}\right)\left(\frac{\dot{m}}{\mathrm{M}_\odot \mathrm{yr}^{-1}}\right). \tag{4}$$

Most of the luminosity will be radiated in the inner 10 R_S over an area $A = \pi(10R_S)^2$. If we assume the emission is black body radiation, we can use the Stefan-Boltzmann law

$$\sigma T^4 = \frac{L}{A} \;\Rightarrow\; T = \left(\frac{L}{A\sigma}\right)^{\frac{1}{4}} = 1.6 \cdot 10^5\mathrm{K} \left(\frac{\dot{m}}{\mathrm{M}_\odot yr^{-1}}\right)^{\frac{1}{4}} \cdot \left(\frac{M_{BH}}{10^8\mathrm{M}_\odot}\right)^{-\frac{1}{2}} \quad (5)$$

where σ is the Stefan-Boltzmann constant to estimate a temperature. With a temperature exceeding 10^5K, the central engine radiates mainly in the ultraviolet.

Hence, a quasar with a luminosity of 10^{46} erg s^{-1} and an efficiency of $\eta = 0.1$ would accrete 1 $\mathrm{M}_\odot\mathrm{yr}^{-1}$. If there is $\sim 10^{10}\mathrm{M}_\odot$ of material in the central region of the galaxy, the lifetime of the quasar would be limited to a few times 10^9 years. Hence, the quasar phase can be just a short fraction of the lifetime of a galaxy.

2.2. THE EDDINGTON LIMIT

The central engine is generating a very large amount of radiation. This radiation exerts a force on the accreting material and sets an upper limit on the luminosity. The Eddington Limit is reached if the radiation force is equal to the gravitational force. The radiation interacts mainly with the electrons, while the gravitation affects predominantly the heavy protons,

$$\frac{\sigma_{th} L}{4\pi R^2 c} < \frac{G M_{BH} m_p}{R^2}. \quad (6)$$

Here is σ_{th} the Thomson cross section for electron photon scattering, L the luminosity, and m_p the proton mass. This requirement gives an lower limit of the black hole mass for a given luminosity assuming isotropic emission:

$$M_{BH} > 0.8 \cdot 10^8\mathrm{M}_\odot \left(\frac{L}{10^{46}\ \mathrm{erg\ s}^{-1}}\right). \quad (7)$$

The Schwarzschild radius of a black hole gives a characteristic size scale and one can calculate an *equivalent* mass density of a black hole:

$$\rho_{BH} = \frac{M_{BH}}{4/3\pi(R_S)^3} = 1.8\ \frac{\mathrm{g}}{\mathrm{cm}^3} \left(\frac{M_{BH}}{10^8 M_\odot}\right) \quad (8)$$

Hence, a black hole with a mass of $5.5 \times 10^7\mathrm{M}\odot$ would have the same *density* as water and a size slightly larger than 1 AU – the size of the Earth orbit. This *density*, of course, should not be taken too serious.

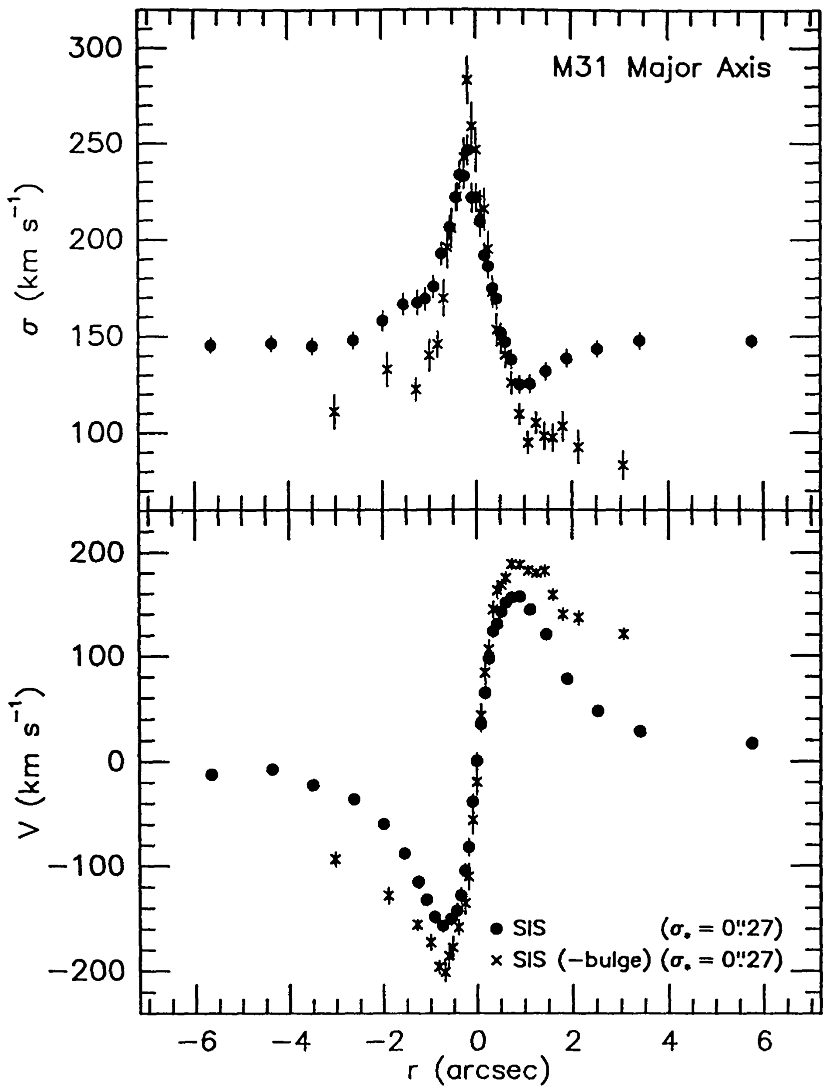

Figure 1. Velocity $V(r)$ (bottom) and velocity dispersion $\sigma(r)$ (top) profiles along the nucleus major axis of M31. (Taken from Kormendy and Richstone 1995).

3. Observational evidence

Black Holes were used to explain the luminous emission of AGN. Quasars are found in many normal galaxies and the AGN-phase is just a short fraction of the lifetime. This leads to the prediction of massive black holes at the center of many galaxies. The fact that accretion onto a black hole

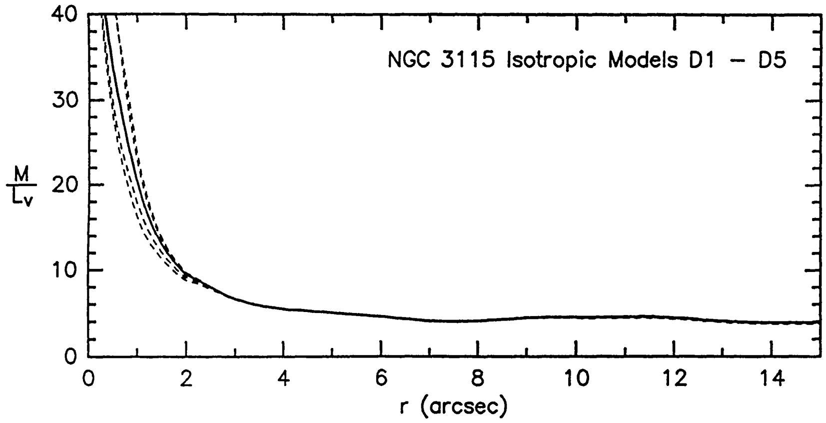

Figure 2. Mass-to-light ratio interior to radius r for NGC 3115. M/L_V increases at $r < 2''$ by a factor of ~ 10 (Taken from Kormendy and Richstone 1995).

can explain the observed luminosities, is no proof for the existence of black holes. To find stronger evidence for supermassive black holes, one has to search for dynamical evidence for *dead quasars* in galaxies. This can be done simplest in nearby galaxies.

3.1. STELLAR VELOCITY DISPERSION

Long-slit spectroscopy of stellar absorption lines in nearby galactic nuclei shows high rotational velocities and a high velocity dispersion towards the center. The velocities are measured from the Doppler shift of the line centroids while the velocity dispersion is inferred from the line width. For an isotropic velocity field with net rotation v and velocity dispersion σ we can derive a central mass of

$$M(r) = \frac{Rv^2}{G} + \frac{R\sigma^2}{G} \tag{9}$$

using essentially the Kepler law and assuming that the stars are virialized.

Figure 1 shows the velocity and velocity dispersion profiles along the nucleus major axis of M31. The velocity dispersion increases towards the center of M31 to ~ 250 km s^{-1} while the velocities increase to ~ 200 km s^{-1} before they drop to 0 km s^{-1} in the center. Kormendy (1988) derived a dark object mass of $\sim 10^7$ M$_\odot$ for this galaxy.

Using formula 9, one can calculate the mass inside a given radius and compare it with the measured stellar light. Figure 2 shows the mass-to-light ratio M/L_V for the galaxy NGC 3115 derived in this way. It stays roughly constant in the outer parts and increases drastically towards the central

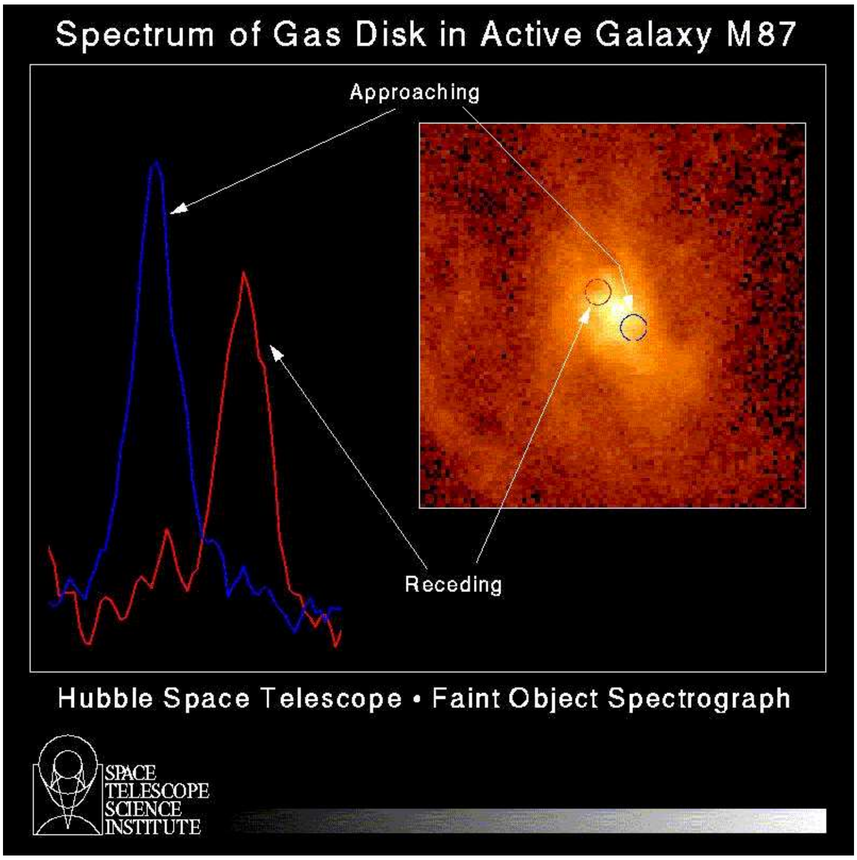

Figure 3. Hubble Space Telescope image of a rotating disk in M87. The emission lines of the receding part are redshifting, while the lines of the approaching part are blue-shifted with respect to the systematic velocity of the galaxy, yielding evidence for a massive dark object – presumably a black hole. (Ford *et al.* 1994)

region of the galaxy. The kinematic data indicates that NGC 3115 harbors a massive dark object with a mass of 10^9 $M_\odot$ (Kormendy and Richstone, 1992) in its center.

3.2. HIGH-RESOLUTION SPECTROSCOPY OF GAS

A further hint for massive matter concentrations comes from the kinematic behavior of the interstellar gas close to the core of galaxies. The Hubble Space Telescope is able to resolve the dynamics of stars and the gas in nearby galaxies. A prime example is the nearby giant elliptical galaxy M87 which contains a hot rotating disk in the center (see Figure 3). Measurements of the radial velocities using spectroscopy of emission lines from

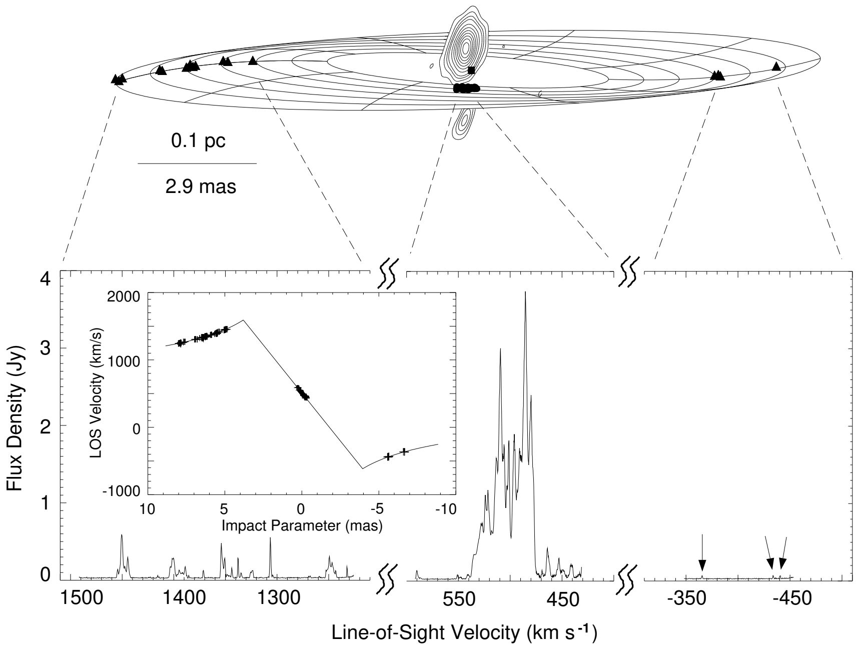

Figure 4. The warped disk model, the maser positions and the 22 GHz continuum emission of a sub-parsec-scale jet from VLBI observations of NGC 4258 (top). Also shown is the total spectrum with masers at the systematic velocity of $\sim$ 470 km s^{-1} and the *high-velocity* masers Doppler shifted by $\pm$1000 km s^{-1}. The inlay shows the line-of-sight velocity versus the the impact parameter for a Keplerian disk with the maser data superposed. (Taken from Herrnstein *et al.* 1999).

the ionized gas show the gas to be in Keplerian rotation about a mass of $M = 2.4 \times 10^9$ M$_\odot$ within the inner 18 pc of the nucleus (Ford *et al.* 1994; Harms *et al.* 1994).

3.3. WATER MASERS – NGC 4258

Strong evidence for a supermassive black hole comes also from interferometric spectral line observations of water vapor maser emission in the centers of galaxies. The spectrum of the H_2O maser emission in the Seyfert galaxy NGC 4258 consists of maser components at the systematic velocity of the galaxy as well as high-velocity masers which are Doppler shifted by $\pm$1000 km s^{-1}. High resolution Very Long Baseline Interferometry (VLBI) observations show the maser spots in a thin warped disk around the center. The masers with the systematic velocity appear in front of the nucleus, while the blue- and red-shifted components are on the approaching and receding sides of the disk which is in perfect Keplerian rotation (Figure 4). From the rotation and the distance of the source, one can estimate an

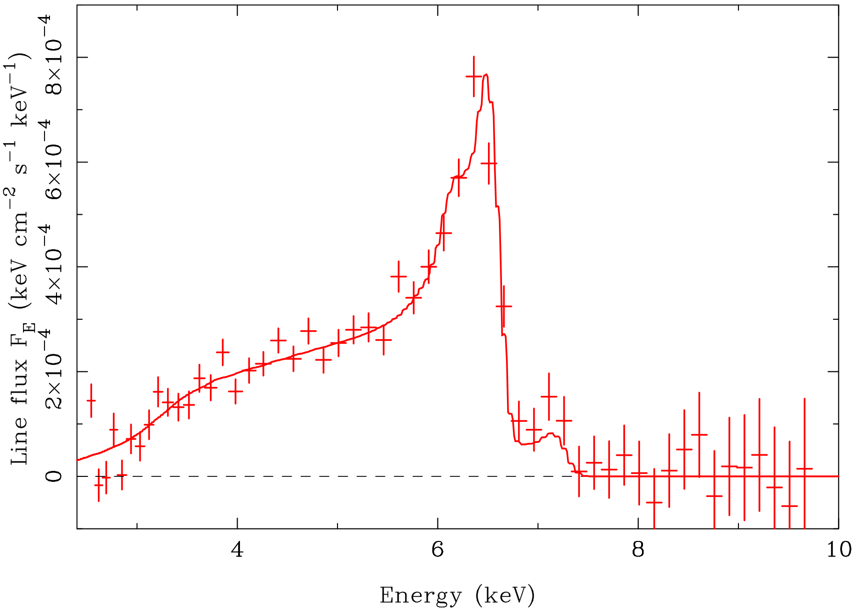

Figure 5. Continuum subtracted relativistic iron line profile from an XMM-Newton observation of MCG-6-30-15 (Taken from Fabian *et al.* 2002).

enclosed mass of $3.6 \times 10^7 M_\odot$ within 0.1 parsecs (Miyoshi *et al.* 1995; Herrnstein *et al.* 1997). This requires a mass density of $> 4 \times 10^9$ $M_\odot pc^{-3}$.

3.4. RELATIVISTICALLY BROADENED IRON Kα-LINE

X-ray spectroscopy of Seyfert galaxies have revealed enormously broadened iron Kα emission lines with line widths of $\sim 100,000$ km s^{-1}. ASCA (Advanced Satellite for Cosmology and Astrophysics) observations by Tanaka *et al.* (1995) found that the iron line profile in MCG-6-30-15 could be explained by emission from an accretion disk around a black hole. Recent XMM-Newton observations (see Figure 5) find also extremely broad and redshifted emission indicating an origin in the central regions of an accretion disk around a rotating black hole (Wilms *et al.* 2002; Fabian *et al.* 2002).

3.5. BLACK HOLES AND THEIR HOST GALAXIES

Many nearby galaxies show evidence for a massive dark object in their center. This raises the question whether the evolution of black holes and galaxies are connected. Hence it is important to search for correlations between properties of the black hole and those of galaxies. Gebhardt *et al.* (2000) and Ferrarese and Merritt (2000) found a strong correlation be-

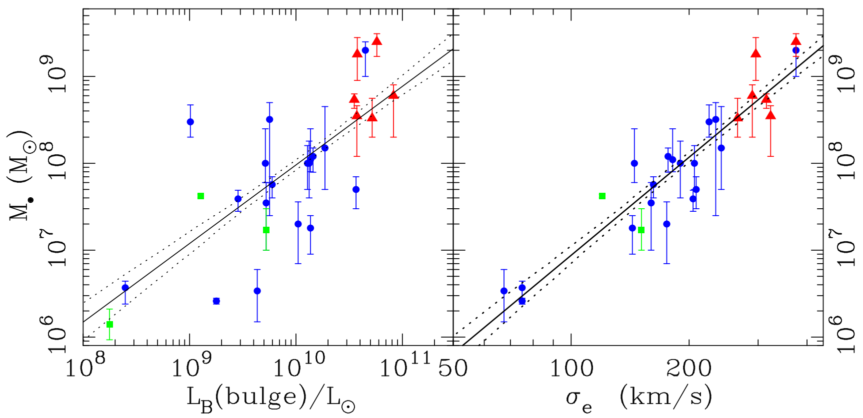

Figure 6. Black hole mass versus bulge luminosity (left) and the velocity dispersion (right). The velocity dispersion shows a tight correlation with the the mass of the cental black hole. Solid and dotted lines are the best fit and their 68% confidence bands. (Taken from Gebhardt et al. 2000).

tween the black hole mass and the velocity dispersion of stars in the bulge of the host galaxy. Figure 6 shows this correlation for 26 galaxies with black hole masses from kinematics of stars, gas and masers.

The velocity dispersion of stars in the bulge depends on the mass of the spheroidal stellar component and this correlation indicates that the more massive the bulge the heavier is the black hole. This suggests that the evolution of black holes and their host galaxies are intimately linked.

There are various processes for bulge and black hole mass evolution. A primordial hydrogen cloud collapses around a small black hole. Infalling gas feeds the black hole and forms stars. Finally the collapse yields a giant elliptical galaxy or bulge and the black hole growth stops. Another scenario is the merger of two spiral galaxies with black holes. The galaxies collide and the merger yields an elliptical galaxy with a larger central black hole. The central black hole could also grow throughout the cosmological history by accretion of ordinary or dark matter through the galactic disk or halo into the center. Hence, while black holes can grow in different ways, the reason why black holes and bulges are so intimately linked remains a big puzzle.

4. The Dark Mass in the Galactic Center

The closest place to look for a supermassive black hole is the center of our own Galaxy. The compact radio source Sgr A* in our Galactic Center is thought to contain a black hole. For a detailed review about the inner parsecs of our Galaxy see Melia and Falcke (2001).

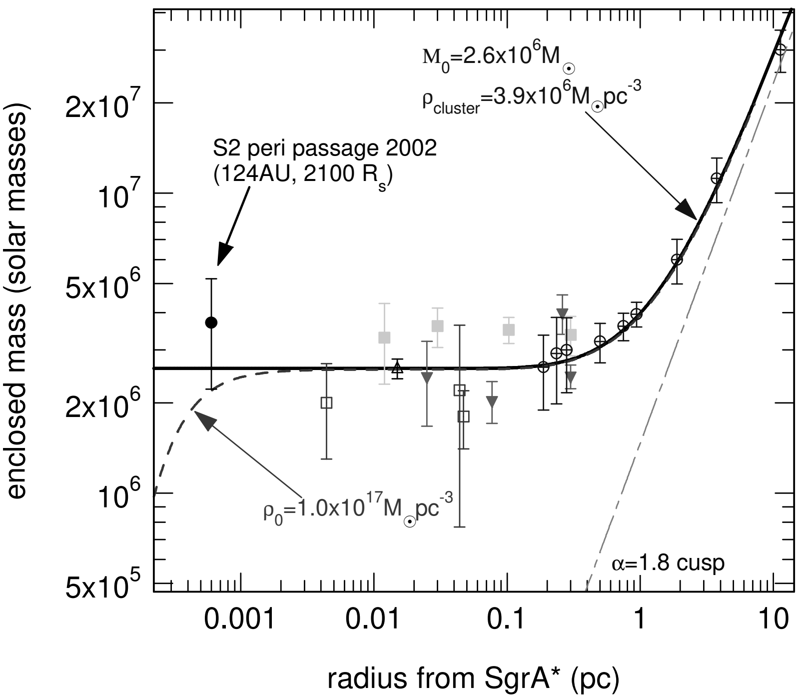

Figure 7. Enclosed mass as a function of radius from Sgr A* in the Galactic Center (Taken from Schödel et al. 2002).

Measurements of stellar proper motions in the vicinity of Sgr A* have revealed a dark mass in the Galactic Center. The center of gravity coincides with Sgr A* within 0.01 light years. Recently Ghez *et al.* (2000) and Eckart *et al.* (2002) detected for the first time acceleration in the proper motions. This allows one to constrain the possible orbits around Sgr A* and locate the center of mass even better.

For one star, both peri- and apo-center passages have been observed recently that show a highly elliptical Keplerian orbit with an orbital period of 15.2 years and a peri-center distance of 17 light hour (Schödel *et al.*, 2002). This orbit requires an enclosed mass of $3.7 \pm 1.5 \times 10^6$ M$_\odot$. Figure 7 shows the enclosed mass as a function of the radius from Sgr A*. The solid curve is the best fit to all data points and represents the sum of a $2.6 \pm 0.2 \times 10^6$ M$_\odot$ point mass and a stellar cluster with central density 3.9×10^6 M$_\odot$ pc^{-3}, core radius 0.34 pc and power-law index $\alpha = 1.8$.

Further evidence about the nature of Sgr A* comes from its proper motion with respect to background quasars that has been measured with VLBI. Sgr A* apparently moves with 219 km s^{-1} along the Galactic Plane (see Figure 8), which entirely reflects the motion of the sun around the

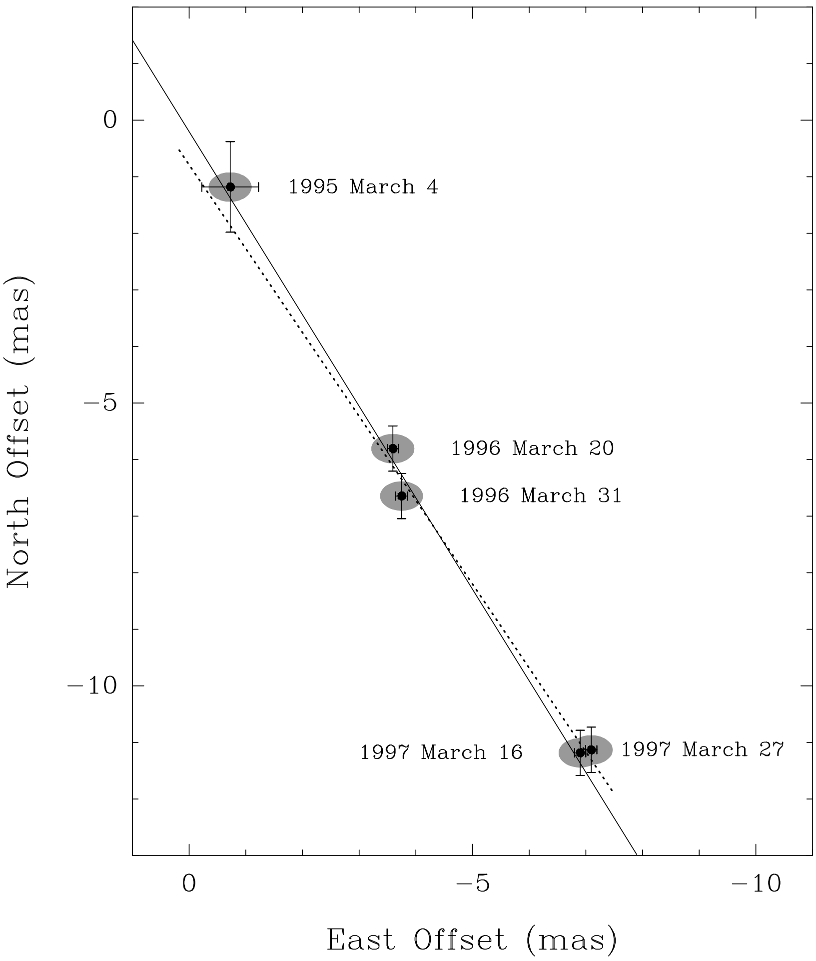

Figure 8. Proper motion of Sgr A* with respect to background quasars measured with VLBI. The solid line gives the orientation of the Galactic plane (Taken from Reid *et al.* 1999).

Galactic Center. Hence the proper motion of Sgr A* itself is consistent with zero (Reid *et al.* 1999; Backer & Sramek 1999). This is in clear contrast to the velocities of stars in the central region which move at speeds that exceed 1000 km s^{-1}. Thus, Sgr A* has to be much more massive than these stars and the upper limit on the speed gives a lower limit on the mass of $\sim 10^3 M_\odot$. Further VLBI observations (Reid and Brunthaler, 2003) and improved theoretical models (Chatterjee, Hernquist and Loeb, 2002) increase the lower limit to $\sim 10^5 M_\odot$.

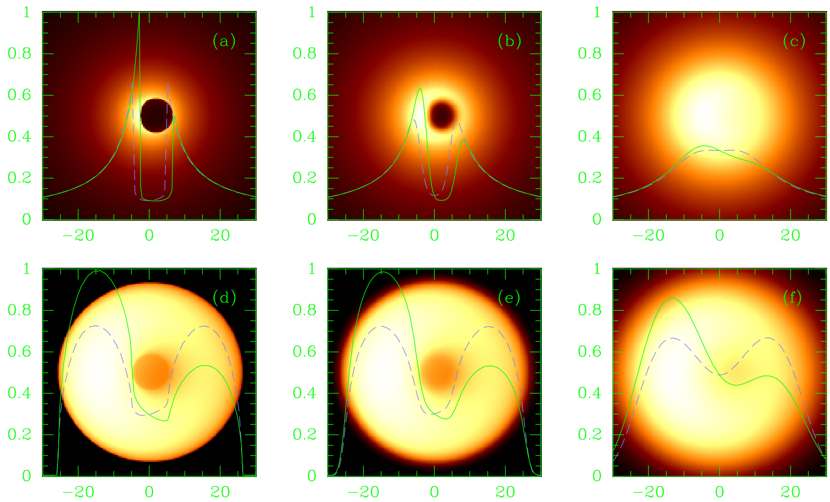

Figure 9. Shadow of a black hole. For a description see text. (Taken from Falcke, Melia and Agol 2000).

Black holes emit strong emission at scales that are affected by General Relativity. The photon orbits are bent in the vicinity of the black hole and can become circular at distances of $\sim 2 - 3R_S$. Closer orbits will end in the event horizon and produce a *shadow* in the emitting region around the black hole. Figure 9 shows the model image of an optically thin emission region surrounding a black hole with the characteristics of Sgr A* at the Galactic Center. The black hole is either maximally rotating (upper row) or non rotating (lower row). Images (a,d) show ray-tracing calculations, (b,e) are the images seen by an idealized VLBI array at 0.6 mm wavelength, taking interstellar scattering into account. The images (c,f) are for a wavelength of 1.3 mm. The intensity variations along the x-axis (solid curve) and the y-axis (dashed curve) are overlayed. For Sgr A*, the predicted size of this shadow is ~ 30 μas and approaches the resolution of current VLBI experiments (Falcke, Melia and Agol, 2000).

Recently Sgr A* was detected for the first time with VLBI at 1.4 mm on one baseline (Plateau de Bure - Pico Veleta). Krichbaum *et al.* (1998) derived a source size of 0.11 ± 0.06 mas or 17 ± 9 Schwarzschild radii for a 2.6×10^6 M$_\odot$ black hole. Figure 10 shows the source size of Sgr A* versus wavelength. The data points follow a λ^2 behavior which is expected from scatter broadening by the interstellar medium. The source size at 1.4 mm is significant larger than the scattering size and may be intrinsic. This size is just a factor of 3 away from the shadow.

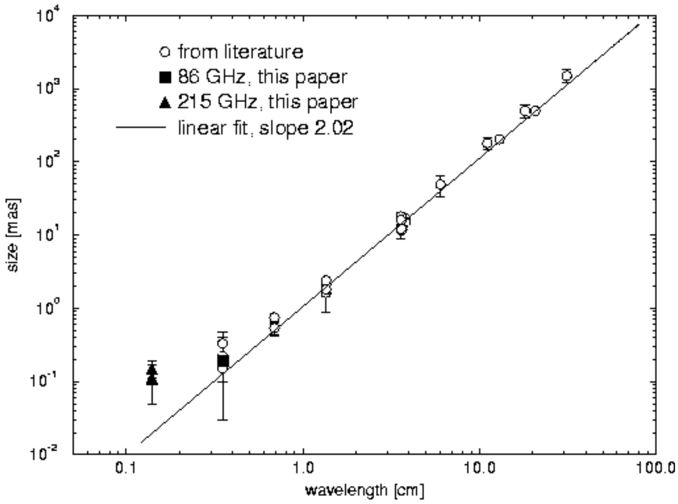

Figure 10. Size of Sgr A* versus observing wavelength. (Taken from Krichbaum et al. 1998).

5. Conclusion

Black holes were introduced into astrophysics as purely theoretical concepts which were needed to explain quasar luminosities. In the last years, strong evidence was found that the nuclei of non-active galaxies harbor large dark point masses. Studies of the properties of the host galaxies show that the evolution of black holes and their host galaxies is closely linked. The best black hole candidates are Sgr A* and NGC 4258 and submm-VLBI will soon approach the event horizon for the black hole in the Galactic Center to finally prove the concept of supermassive black holes.

References

Backer, D.C. and Sramek, R.A. 1999, ApJ 524, 805
Chatterjee, P., Hernquist, L. and Loeb, A. 2002, ApJ 572, 371
Eckart, A. and Genzel, R. 1996, Nature 383, 415
Eckart, A., Genzel, R., Ott, T., and Schödel, R., 2002, MNRAS 331, 917
Fabian, A.C. et al. 2002, MNRAS 335, L1
Falcke, H., Melia, F. and Agol, E. 2000, ApJ 528, L13
Ferrarese, L. and Merritt, D. 2000, ApJ 539, L9
Ford, H.C. et al. 1994, ApJ 435, L27
Gebhardt, K. et al. 2000, ApJ 539, L13
Ghez, A.M., Morris, M., Becklin, E.E., Tanner, A. and Kremenek, T. 2000, Nature 407, 349
Harms, R.J. et al. 1994, ApJ 435, L35
Hazard, C., Mackey, M.B. and Shimmins, A.J. 1963, Nature 197, 1037

Herrnstein, J.R., Moran, J.M., Greenhill, L.J., Diamond, P.J., Miyoshi, M., Nakai, N. and Inoue, M. 1997, ApJ 475, L17

Herrnstein, J.R., Moran, J.M., Greenhill, L.J., Diamond, P.J., Inoue, M., Nakai, N., Miyoshi, M., Henkel, C. and Riess, A. 1999, Nature 400, 539

Kormendy, J. 1998, ApJ 325, 128

Kormendy, J. and Richstone, D. 1992, ApJ 393, 559

Kormendy, J. and Richstone, D. 1995, ARAA 33, 581

Krichbaum, T.P. et al. 1998, A&A 335, L106

Melia, F. and Falcke, H. 2001, ARAA 39, 309

Miyoshi, M., Moran, J., Herrnstein, J., Greenhill, L., Nakai, N., Diamond, P. and Inoue, M. 1995, Nature 373, 127

Reid, M.J., Readhead, A.C.S., Vermeulen, R.C. and Treuhaft, R.N. 1999, ApJ 524, 816

Reid, M., and Brunthaler, A. 2003, to be published in Astron. Nachr., Vol. 324, No. S1 (2003), Special Suplement "The central 300 parsecs of the Milky Way", Eds. A. Cotera, H. Falcke, T. Geballe, S. Markoff

Schmidt, M. 1963, Nature 197, 1040

Schödel, R. et al. 2002, Nature 419, 694

Tanaka, Y. et al. 1995, Nature 375, 659

Wilms, J., Reynolds, C.S., Begelman, M.C., Reeves, J., Molendi, S., Staubert, R., and Kendziorra, E. 2001, MNRAS 328, L27